

Microstrip Discontinuities on Cylindrical Surfaces

Jifu Huang, Ruediger Vahldieck and Hang Jin

Laboratory for Lightwave Electronics, Microwaves and Communications
 (LLiMiC)
 Department of Electrical and Computer Engineering
 University of Victoria
 Victoria, B.C., V8W 3P6, Canada

Abstract

S-parameter analysis of microstrip discontinuities on cylindrical dielectric surfaces is presented using the full-wave frequency-domain TLM method. Microstrip step and gap discontinuities on the same side of the substrate as well as overlay coupling of two microstrip lines on opposite sides of the substrate are investigated. The finite conductor thickness is taken into account as well as the interaction of higher order modes between cascaded discontinuities.

Introduction

Microstrip transmission lines on curved surfaces are of importance as feed lines for radiators on cylindrical surfaces. Considerable work has been done analyzing a variety of those structures with different methods. However, all this work is limited to the calculation of the propagation constant and characteristic impedance (i.e. [1-2]). Furthermore, most of the data available is based on quasi-static analysis and does not take into account dispersion effects.

In this paper a rigorous analysis is presented using the frequency-domain TLM (FDLTM) method which has been published recently by Jin and Vahldieck [3] for rectangular structures. In this paper we expand the theory presented in [3] to the analysis of cylindrical microstrip step and gap discontinuities. This includes overlay coupling between two microstrip transmission lines on opposite sides of the substrate. Furthermore, while in [3] still a 15-port symbolic s-matrix was used in the TLM network, the present algorithm is based on a 12-port symbolic s-matrix.

Theory

The FDLTM is a universal full-wave frequency-domain simulation tool which can be applied to rectangular or circular cross-sections. To analyze cylindrical structures, a cylindrical mesh based on the symmetrical condensed TLM node is used to avoid approximation of curved surfaces by a rectangular mesh. The node used in the following analysis is shown in Fig.1(a). Since in the frequency-domain time synchronism is not required, the stubs in the condensed node used in an earlier approach can be eliminated. Therefore the size of the node symbolic s-matrix is reduced to that of a 12-port. By further assuming that the characteristic admittance of each transmission line branch is the same and equals the intrinsic admittance of the medium occupying the node, the symbolic s-matrix is given as shown in Fig.1(b). The coefficients of symbolic s-matrix are reduced to $a_n=c_n=0$, $b_n=d_n=1/2$. The normalised propagation constants on the cylindrical transmission line mesh are given as:

$$\begin{aligned}\tilde{\gamma}_r &= \frac{1}{2} \left(\frac{(r\alpha)^2 + v^2}{r\alpha \cdot v} - \frac{r\alpha \cdot v}{u^2} \right) \\ \tilde{\gamma}_\theta &= \frac{1}{2} \left(\frac{u^2 + v^2}{u \cdot v} - \frac{u \cdot v}{(r\alpha)^2} \right) \\ \tilde{\gamma}_z &= \frac{1}{2} \left(\frac{u^2 + (r\alpha)^2}{u \cdot r\alpha} - \frac{u \cdot r\alpha}{v^2} \right)\end{aligned}\quad (1)$$

where u , $r\alpha$, and v are the dimensions of the node in r , θ , and z directions, respectively.

The objective is to compute the scattering parameters of a 3-D discontinuity region of cylindrical shape. This requires the computation of the incident, reflected and transmitted modes at the reference planes of a discontinuity region. The algorithm of the FDLTM is based on the concept of



the *intrinsic scattering matrix*, which is, in general, defined as the coefficient matrix relating the reflected and incident waves at the exterior branches of a TLM network. An explicit expression for the intrinsic scattering matrix has been given in [3] in terms of the scattering matrix S and connection matrix C of the TLM network. Once the intrinsic scattering matrix is known, all the properties of the structures can be computed through matrix operations. A brief description of this algorithm will be given for the case of a two port circular discontinuity problem, which consists of a discontinuity region and two attached semi-infinity waveguides as input and output ports. First we find the intrinsic scattering matrices for the discontinuity region and the two attached semi-infinity waveguides. They are denoted m , R_1 and R_2 , respectively. The incident and reflected modes at the interfaces to the discontinuity region and the attached waveguides are related as follows:

$$\begin{pmatrix} b_1 \\ b_2 \end{pmatrix} = m \cdot \begin{pmatrix} a_1 \\ a_2 \end{pmatrix} = \begin{pmatrix} m_{11} & m_{12} \\ m_{21} & m_{22} \end{pmatrix} \cdot \begin{pmatrix} a_1 \\ a_2 \end{pmatrix} \quad (2)$$

where a_1, b_1 are the incident and reflected mode vectors at the interface of waveguide one and the discontinuity region; while a_2, b_2 are the incident and reflected mode vectors at the interface of waveguide two and the discontinuity region (each element of these vectors corresponds to one branch of the network). The excitation of the system, a_{10} and b_{10} , which is obtained from a two dimensional analysis[3], is incident at the interface between waveguide one and the discontinuity region. It should be noted that vector a_{10} and b_{10} describe the field distribution over the cross-section of waveguide one. The reflected waves, a_1', b_1' , at waveguide one are then given by

$$a_1' = R_1 \cdot b_1' \quad (3)$$

$$b_1' = (I - R_2' \cdot R_1)^{-1} \cdot (R_2' - R_1) \cdot a_{10} \quad (4)$$

where R_2' :

$$R_2' = m_{11} + m_{12} \cdot R_2 \cdot T' \quad (5)$$

$$T' = (I - m_{22} \cdot R_2)^{-1} \cdot m_{21} \quad (6)$$

a_2, b_2 at waveguide two are obtained from:

$$a_2 = R_2 \cdot b_2 \quad (7)$$

$$b_2 = T' \cdot a_1 = T' \cdot (R_1 \cdot b_1' + a_{10}) \quad (8)$$

From (4)~(8), the corresponding s-parameters can be obtained [3].

Results

In the following analysis the metallization thickness is always considered and assumed to be $3\mu\text{m}$. Fig.2 is a simple step discontinuity and the calculated s-parameters are shown as a function of frequency. A cylindrical substrate with inner and outer radii $r_1=4$ mm and $r_2=4.25$ mm, respectively, and relative dielectric constant $\epsilon_r=10$ is used. Like in a planar structure, the results are quite flat over a large frequency range indicating very little dispersion. The typical computation time in this case is approximately 15 seconds for one frequency point on a SUN SPARC II station. For a gap discontinuity on a substrate with inner and outer radii $r_1=10.0$ mm and $r_2=10.635$ mm, respectively, the s-parameters are illustrated in Fig.3. The gap width is $g=0.2$ mm. Also here the s-parameters behave similar to a structure on a plane substrate. Fig.4 shows the frequency-dependent s-parameters for a transition of magnetically coupled microstrip lines on opposite sides of the substrate. Three different overlap lengths are considered: $d=0.5$ mm, $d=1.5$ mm, and $d=3.0$ mm. As expected, the longer the overlap length the lower the frequency at which the optimum match occurs. For example for $d=3$ mm the minimum S_{11} occurs at about 15GHz while for $d=0.5$ mm it occurs at frequencies higher than 40 GHz.

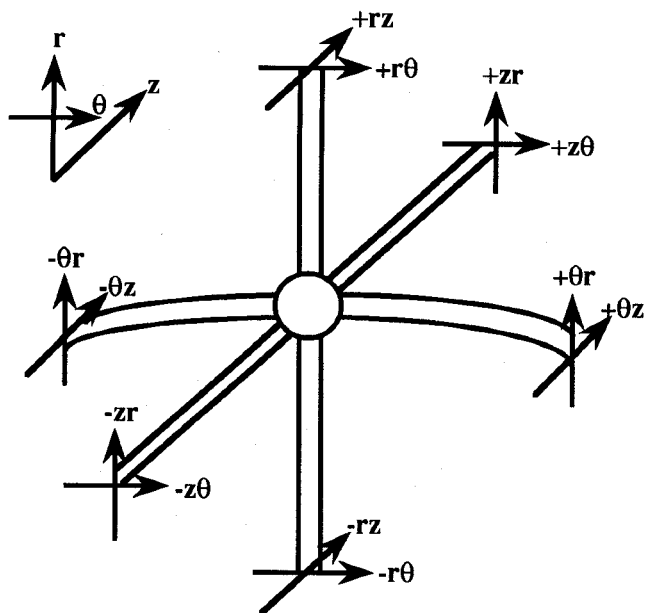
Conclusions

We have introduced a frequency-domain TLM algorithm for a circular coordinate system using a 12-port symbolic s-matrix. Based on this algorithm then scattering parameters for microstrip discontinuities on curved surfaces have been investigated.

References

- [1] L.R.Zeng, and Y.Wang, "Accurate solutions of elliptical and cylindrical striplines and microstrip lines", *IEEE Trans. Microwave Theory Tech.*, vol. MTT-34, pp. 259-265, 1986.
- [2] N.G.Alexopoulos and A.Nakatani, "Cylindrical substrate microstripline characterization," *IEEE Trans. Microwave Theory Tech.*, vol. MTT-35, pp. 843-849, 1987.

[3] H. Jin and R. Vahldieck, "The frequency domain TLM method - A new concept", IEEE Trans. Microwave Theory and Tech. vol.40, No.12, Dec. 1992, pp.2207-2218.



(a)

Column Number		Row Number									
		+rθ	+rz	-rθ	-rz	+θr	-θr	-zr	+zr	+zθ	-zr
+rθ	a_3	c_3		d_1	$-d_1$	b_4	b_4				
+rz	a_6	c_6	b_5	d_1	b_5	d_2	d_2	b_4			
-rθ	c_3	a_3		d_1	d_1	b_4		d_2	b_4		
-rz	c_6	a_6	b_5		b_5	d_2	d_2	d_4			
+θr	b_6	b_6	a_5		c_5	c_1	b_2		b_2	d_4	
-θr	d_3	d_3	b_6	c_5	a_5	c_1	b_2	$-d_4$	b_2	d_4	
-zr	d_6	d_6	d_6	c_5	c_5	a_1	b_2		b_2		
+zr	d_3	d_3	d_6	b_1	d_1	b_1	a_2		c_2		
+zθ	b_3	b_3	d_5	b_1	d_5	b_1	c_2	a_4		c_4	
-zr	d_6	d_6	d_6	b_1	d_5	b_1	c_2	c_4	a_2		
-zθ	b_3	b_3	d_5	d_5	b_1	b_1	c_2	c_4	a_4		

(b)

Fig. 1 (a) Symmetric condensed node for cylindrical geometry; (b) Symbolic scattering matrix

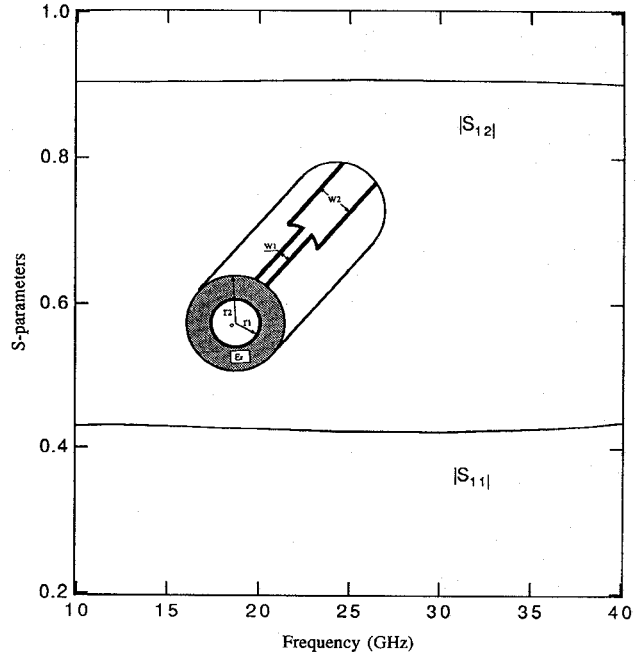


Fig.2 Frequency-dependent S-parameters of microstrip step-in-width. ($r_1=4$ mm, $r_2=4.25$ mm, $\epsilon_r=10$, $w_1/(r_2-r_1)=1.0$, $w_2/w_1=4.0$)

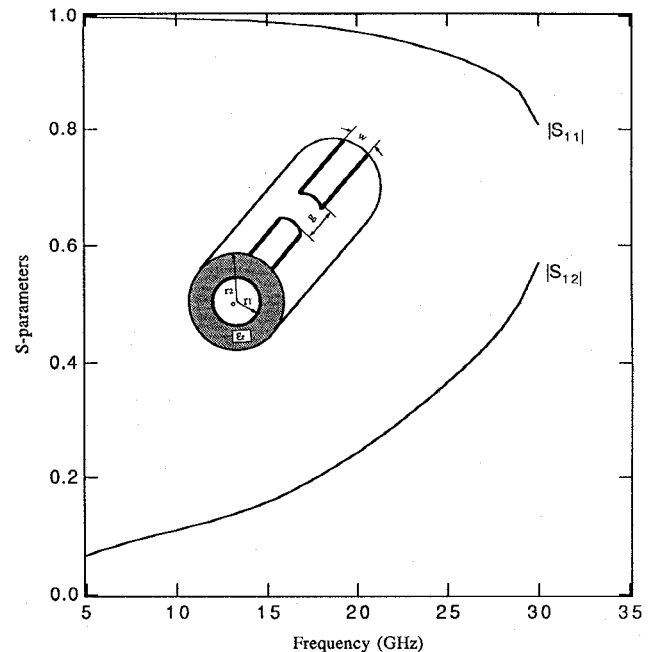


Fig.3 Frequency-dependent S-parameters of microstrip gap discontinuity. ($r_1=10$ mm, $r_2=10.625$ mm, $w=0.635$ mm, $g=0.2$ mm, $\epsilon_r=10$)

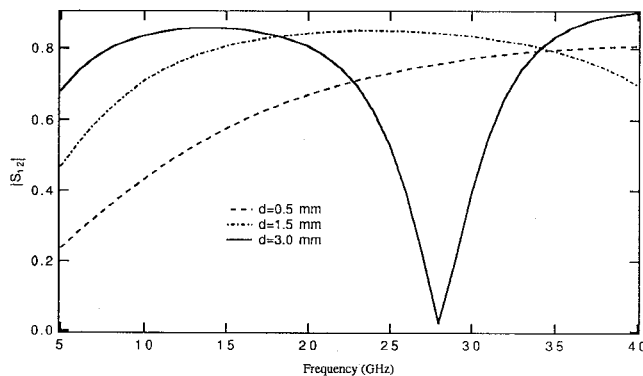
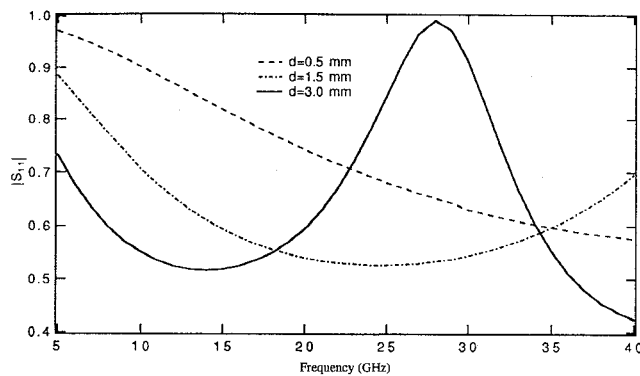
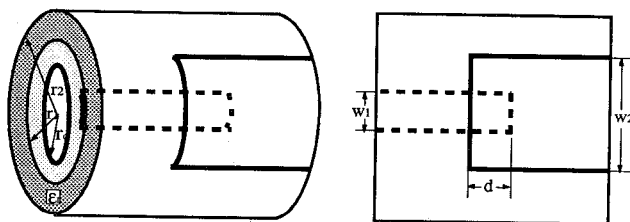


Fig.4 Frequency-dependent S-parameters of microstrip transition on two sides of the substrate. ($r_1=4$ mm, $r_2=4.25$ mm, $\epsilon_r=2.2$, $w_1/(r_2-r_1)=1.0$, $w_2/w_1=4.1$)